euspen's 20th International Conference & Exhibition, Geneva, CH, June 2020
www.euspen.eu

Microscopic behaviour of positioning mechanism driven by preloaded ball screw with external disturbance from ultraprecision turning process

Shigeo Fukada[1], Soichiro Koike[1], Shodai Hirokawa[1]

[1]*Shinshu University, Japan*

sfukada@shinshu-u.ac.jp

Abstract
To determine ultimate positioning performance of a ball screw under practical conditions equivalent to those of positioning mechanisms used in machine tools, microscopic behaviour of the positioning mechanism driven by a preloaded ball screw is here discussed experimentally in externally loaded condition from actual ultraprecision turning process. The experimental apparatus used in previous reports was revised into a two axes positioning mechanism consisting of an X-axis with an aerostatic spindle, and a Z-axis with a diamond cutting tool, resulting in an ultraprecision face lathe. First, micro-step positioning property was measured under constant axial load applied by a voice-coil-type actuator. Fine positioning with 50 nm step height was realised even with external axial load. Next, similar experiments were performed using actual turning process: It was confirmed that the Z-stage displacement followed the reference of 50 nm step height accurately, and the ball screw operated under nonlinear elastic conditions. Surface topography measurement showed a profile with 50 nm step formed on the surface of the turned workpiece.

Keywords: Ultraprecision positioning, Ball screw, Nonlinear elastic property, Ultraprecision turning

1. Introduction

Ball screws are commonly applied to positioning mechanisms, and are especially used in machine tools requiring both precise motion and high stiffness in case of external disturbances from the machining process. Positioning mechanisms driven by preloaded ball screws have specific elastic properties in microscopic range, which is quite different from the properties in macroscopic rolling condition. Figure 1 shows previous development of author's research on the microscopic behaviour of the preloaded ball screws, and followed by further aspects of the study. In previous reports, various experiments were performed on the microscopic behaviour of ball screws. It was clarified that the ball screws showed nonlinear elastic behaviour within a range of several micrometres: This elastic property was available in the ultra-fine positioning since the displacement revealed no sticking peculiar to the Coulomb's friction, and the ultraprecision positioning with sub-nanometre level resolution was realised by adapting a control system matching the nonlinear elastic property [1, 2]. However, in those experiments, the positioning occurred without any axial load. In order to apply the ultrafine positioning to machine tools, it is necessary to consider the properties under external axial load [3]. In this report, to clarify more practical microscopic behaviour of the positioning mechanism driven by a preloaded ball screw, the properties are discussed on the experiments with external disturbances from the actual ultraprecision turning process, where mutual action and reaction exist between the tool tip on the positioning mechanism and the material of the workpiece, which causes external force acting on the mechanism as disturbances.

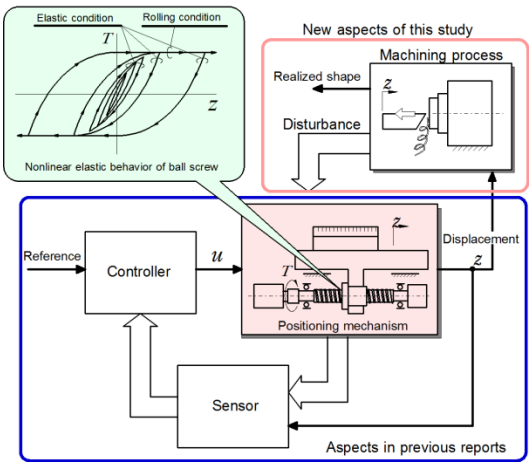

Figure 1. Positioning mechanism under processing

2. Experimental apparatus

2.1. Concept of experiments

Figure 2 shows the concept of the experiments in this report.

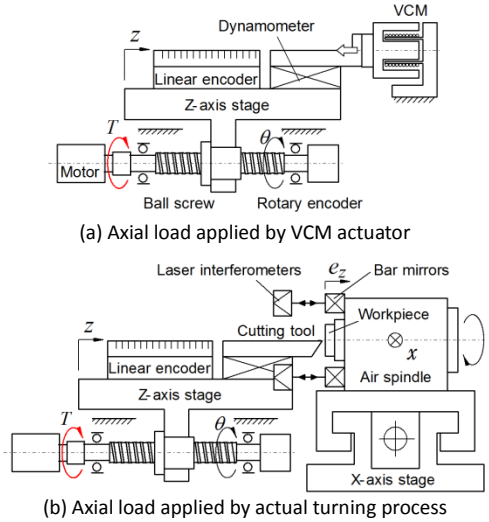

(a) Axial load applied by VCM actuator

(b) Axial load applied by actual turning process

Figure 2. Concept of experimental apparatus

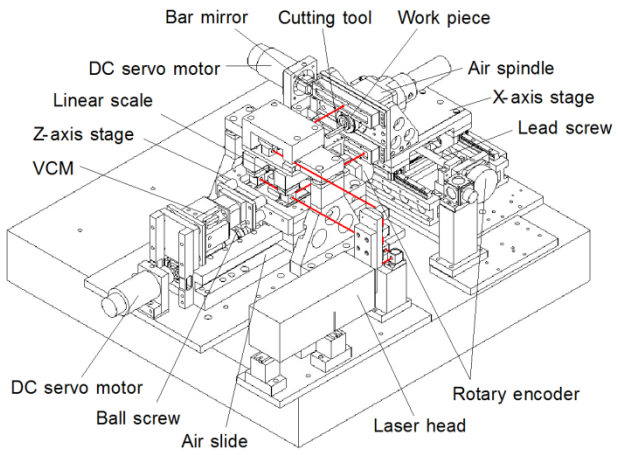

Figure 3. Experimental apparatus

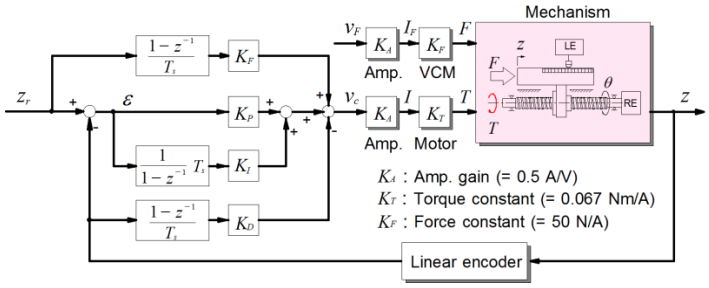

Figure 4. Control system

To discuss the microscopic property under external axial load, an experimental apparatus was devised. It is equipped with a voice-coil-type actuator (VCM) applying axial force to the stage, as shown in Fig. 2(a). First in this report, the property during micro-step positioning was measured under constant axial load applied by the VCM. Next, similar experiments were performed using the actual turning process. The experimental apparatus used in previous reports was revised into two axes positioning mechanism consisting of an X-axis with an aerostatic spindle, and a Z-axis with a diamond cutting tool. This resulted in a simplified ultraprecision face lathe, as shown in Fig. 2(b). And a similar micro-step positioning property was measured under the condition with external disturbances from the ultraprecision turning process.

2.2. Structure of two axes positioning mechanism

Figure 3 shows the experimental apparatus. It consists of two linear positioning stages arranged in orthogonal direction of X and Z axes. The Z-axis stage is identical to the one used in previous experiments [3]. It was supported by an aerostatic guide-way with a stroke of 100 mm, and was driven by a preloaded ball screw with a lead of 5 mm. The preload was applied by over-sized balls with four points of contact around a ball. The ball screw was rotated by a DC servo motor of 130 W, and the motor was driven by a linear current amplifier. The X-axis stage was supported by rolling-type guide ways, and it was driven by a sliding leadscrew. To construct a simplified ultraprecision face lathe, an aerostatic spindle was set on the X-axis stage, and a diamond cutting tool held by a dynamometer detecting thrust force was set on the Z-axis stage. A VCM was set on the opposite side from the cutting tool to apply axial load onto the Z-stage. A linear encoder with resolution of 0.069 nm measured Z-axis displacement. According to Abbe's principle, the measurement axis of the linear encoder coincides with the tip of the cutting tool. To compensate for run-out of the aerostatic spindle caused by straightness error motion of the X-axis, three axes of laser interferometric measurement system were used to measure the motion of two bar mirrors set on the spindle [4]. Those laser measurement axes are set around the detector of the linear encoder and the tool axis, and the value of run-out at the cutting point is derived by processing the measurement values of the three axes.

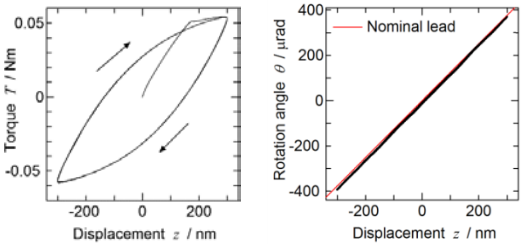

(a) $T-z$ relation (b) θ - z relation

Figure 5. Nonlinear elastic behaviour over 600 nm range

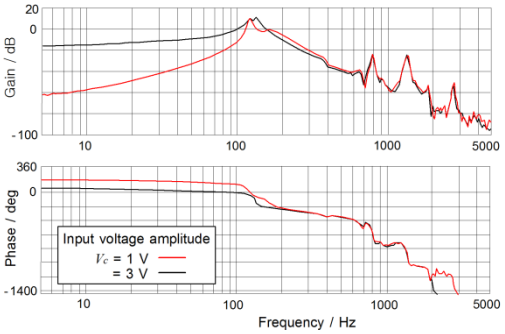

(a) Open loop (from v_c to stage acceleration $\ddot{z}$)

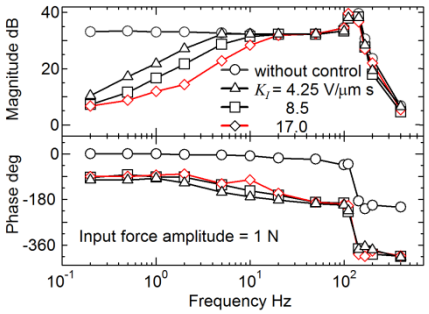

(b) Closed loop (from F to displacement deviation ε)

Figure 6. Frequency response

2.3. Control system

Figure 4 shows the control system of Z-axis, which is a simple PID based control system [2]. The controller has both feedback and feedforward compensators, and it is realised by using a digital signal processor with sampling rate of 8 kHz.

3. Positioning property of Z-axis stage

3.1. Nonlinear elastic property without axial load

As discussed in previous reports, the Z-axis stage shows nonlinear elastic behaviour within microscopic range smaller than several micrometres [2, 3]. Figure 5 shows the property over the range of 300 nm. (a) shows the relation between the motor torque T and the stage displacement z when the screw shaft is rotated quasi-statically to follow a sinusoidal reference with a period of 12 s. It shows nonlinear elastic property with hysteresis. On the other hand, (b) shows the relation between the rotational angle of the screw shaft and stage displacement. It maintains linear relations along the nominal lead of the screw even in these microscopic ranges.

3.2. Frequency response

Figure 6 shows the dynamic property of the Z-axis stage in frequency domain. (a) shows the open-loop frequency response of the mechanism from voltage input to the motor amplifier to output of the stage acceleration [5]. It includes two results with different input voltage amplitudes, 1 V and 3 V, to

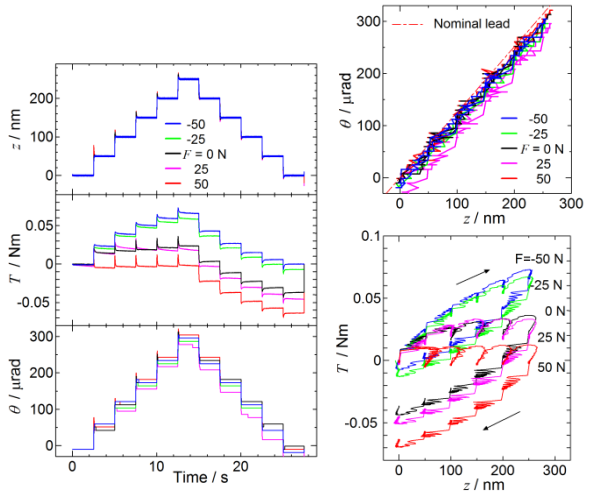

(a) Time domain response (b) $T-z$ relation and $\theta-z$ relation

Figure 7. 50 nm step response of Z-axis under axial load

the amplifier. When the amplitude is above 3 V, the motor rotates macroscopically; when the amplitude is smaller than 1 V, the motion is within the range of nonlinear elastic property. The first resonance is at 130 Hz, and several higher order resonances appear over 400 Hz. Next, to confirm the robustness of the control system, a disturbance response test was performed. Fig. 6(b) shows closed-loop frequency response from the external disturbance input, applied by the VCM, to the output of the stage displacement controlled by the system shown in Fig. 4. The amplitude of the disturbance is 1 N. Response without control is also shown in the figure. Under about 20 Hz, the influence of the disturbance is suppressed by integral operation when Ki is 17.0 V/μm・s. Under the condition with the chosen PID parameters, the break frequencies f_1 and f_2 of the PID property are at approximately 80 Hz and 160 Hz, while the crossover frequency of the loop transfer function is about 14 Hz. Those values ensured the stability of the system.

3.3. Step positioning under constant disturbance

Next, micro step positioning was performed in the Z-axis stage under constant axial disturbance applied by the VCM. Figure 7 shows the experimental results. (a) shows positioned results following the micro multi-step reference with step height of 50 nm under various axial loads. It was confirmed that ultra-fine positioning with a step height of 50 nm was realised under a constant axial load. Fig. 7(b) shows the relations between motor torque *T*, stage displacement *z* and rotation angle θ. The curves in *T*-*z* relation show nonlinear elastic behaviours where the motor torque changes along hysteresis curves, similar to those in Fig. 5(a). And the hysteresis curves shift upper and lower to compensate for the mechanical work in the axial load. Moreover, θ-*z* relations mostly keep a linear relation under a constant axial load.

4. Properties in actual turning process

4.1. Experimental method

In the previous section, it was confirmed that the Z-axis stage realises ultrafine positioning of 50 nm under constant axial loads. In this section, positioning performance is discussed under actual external disturbance from the ultraprecision turning process. Figure 8 shows configuration of the workpiece and experimental method. The workpiece is made of aluminium alloy A5052, and it has cylindrical configuration with outer diameter of 38 mm; its end surface was turned using a diamond cutting tool with nose radius of 0.76 mm [6]. Table 1 shows the cutting condition. To form a step profile in radial direction on the end surface, a multi-step motion command

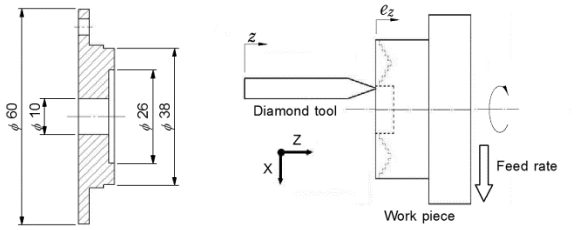

(a) Configuration of workpiece (b) Cutting motion

Figure 8. Workpiece and cutting motion

Table 1. Cutting condition

Revolution speed rpm	1500
Cutting speed m/min	155
Cutting depth μm	1
Feed rate μm/rev	10
Cutting tool	Diamond
Nose radius mm	0.76
Work material	A5052

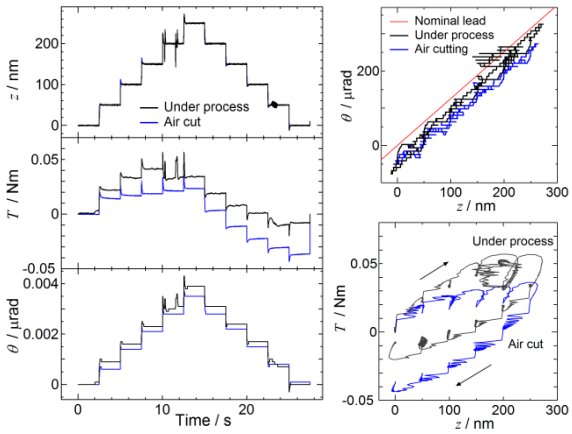

(a) Time domain response (b) $T-z$ relation and $\theta-z$ relation

Figure 9. 50 nm step response of Z-axis under machining

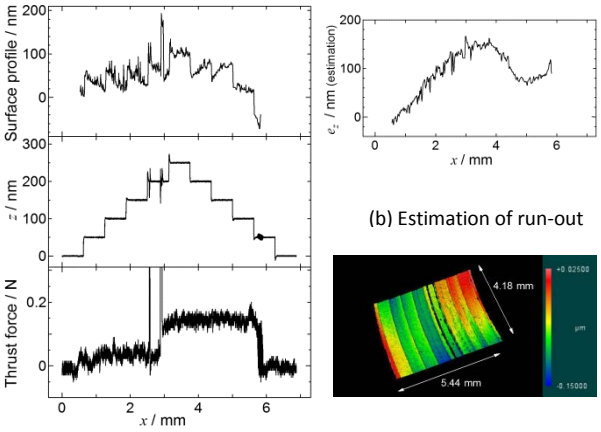

(a) Space domain profile and thrust force (c) Surface topography

(b) Estimation of run-out

Figure 10. Surface profile after 50 nm step machining

was applied to the Z-axis carrying the diamond tool, while the X-stage fed the spindle at a constant feed rate.

4.2. Cutting under simple step motion of Z-stage

First, the workpiece was machined by turning under a simple step motion of the Z-stage with height of 50 nm, similar to the experiments in Fig. 7. Fine cutting under the condition in Table 1 was performed several times repeatedly in the same condition after rough cutting. Figure 9 shows the response of the Z-axis stage in time domain during final fine cutting. The motion of the stage follows the reference with 50 nm step height accurately even in cases of actual external disturbance from the turning. *T*-*z* relation in Fig. 9(b) follows curves similar to nonlinear elastic behaviour shown in Fig. 7 on the

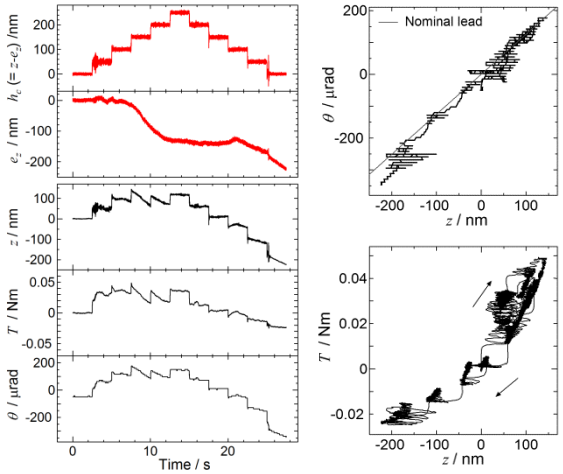

(a) Time domain response (b) $T-z$ relation and $\theta-z$ relation

Figure 11. 50 nm step response of cutting depth under machining

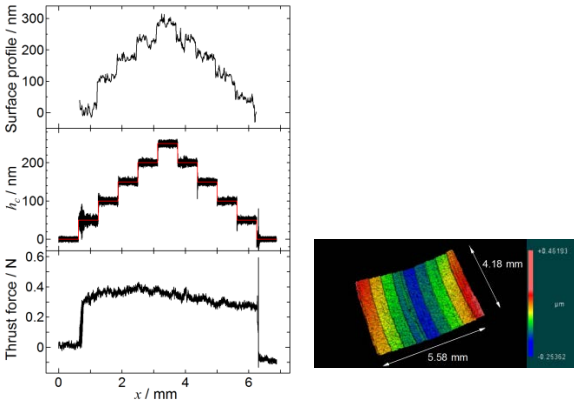

(a) Space domain profile and thrust force (b) Surface topography

Figure 12. Surface profile after compensated 50nm step machining

experiments under constant disturbance, compared with the property without axial load in air cut. The curve shifts upward to compensate for the mechanical work for thrust force by turning. Moreover, z-θ relation in Fig. 9(b) shows a near-linear relation under the actual cutting condition.

Figure 10 shows the space domain profile of the Z-axis motion, i.e. the tool motion, and the machined surface, with thrust force during the cutting. Though the profile of the tool motion accurately follows the step command, the surface profile does not agree with the tool motion. Fig. 10(b) shows a difference between the tool motion and the surface profile: It shows relatively smooth change over the travel range with amplitude less than 200 nm. It was estimated that this discrepancy was affected by the run-out motion of the spindle caused by a straightness error in the X-axis motion. Fig. 10(c) shows surface topography obtained by a laser coherence scanning interferometry microscope: This shows that the step configuration was not uniform over the measured area.

4.3. Compensation of straightness error of X-axis (real cutting depth control)

In the previous section, it was shown that the straightness error motion of the X-axis stage negatively affected the transcription accuracy from tool motion to surface profile. This experimental apparatus has a measurement system that detects run-out motion of the spindle, as mentioned above. To control actual cutting depth by compensating for the error motion of the spindle, a new control system was devised. The actual cutting depth h_c is given by the following equation [7]:

$$\begin{cases} e_z = E_{ZX} + E_{BX}\,x \\ h_c = z - e_z \end{cases} \quad (1)$$

where z is the displacement of the Z-axis stage, and e_z is run-out of the spindle. The Z-axis displacement was controlled

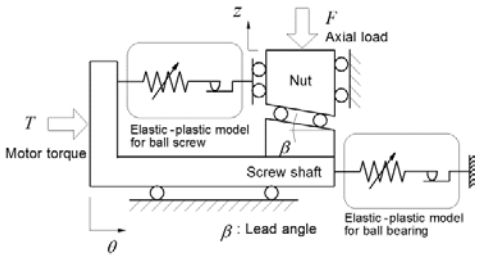

Figure 13. Mechanical model

through real-time operation by correcting the reference value z_r in the block diagram in Fig. 4 to compensate for the e_z detected by the laser measurement system.

Figure 11 shows the response of the Z-axis stage in time domain during the final fine machining. In this case, the Z-axis displacement was modified as such without uniform steps of 50 nm to compensate for the run-out of the spindle over 200 nm. By the compensation, relative displacement between the tool and the spindle, i.e. the actual cutting depth, was controlled by uniform steps with a height of 50 nm. The T-z relation in (b) also shows nonlinear elastic behaviour, while the z-θ relation maintains the linear. Figure 12 shows the space domain profile of the actual cutting depth and the machined surface, with thrust force. The step profile of the machined surface was improved by compensating for run-out motion of the spindle, while the surface topography in (b) shows regular change of height of band areas in the radial direction.

On the basis of the above experimental results, it was confirmed that the positioning mechanism driven by a preloaded ball screw has a superior performance for ultraprecision positioning, even under external disturbance from ultraprecision machining, which realises machining with several tens of nanometre resolution. Figure 13 shows the proposed mechanical model for the microscopic behaviour of the ball screw mechanism with support bearing [1]. The axial force applied to the stage maintains its equilibrium under nonlinear elastic conditions, and the rotation of the screw shaft is transmitted into the nut displacement along the geometric lead angle of the screw within these microscopic ranges of nanometres. This superior property of the ball screw results in ultrafine machining.

5. Conclusion

To clarify the microscopic behaviour and positioning property under external disturbance from the actual ultraprecision turning process, experiments on the positioning mechanism driven by a preloaded ball screw were performed in both cases of using constant axial load and actual machining conditions. The ball screw showed nonlinear elastic behaviour under the external disturbance from ultraprecision turning process. And it was proved that its superior positioning performance was kept in the nanometre range even under external axial disturbances, so that ultraprecision machining with resolution of several tens of nanometres was realised.

References

[1] Fukada S, Fang B and Shigeno A 2011 *Prec. Eng.* **35** 650-68
[2] Fukada S, Matsuyama M and Hirayama J 2012 *Proc. euspen 12th Int. Conf.* 306-310
[3] Fukada S and Koike S 2017 *Proc. euspen 17th Int. Conf.* 449-450
[4] Gao W, Tano M, Kiyono S, and Park C H 2007 *Prec. Eng.* **31** 310-316
[5] Fukada S, and Shimura T S *Proc. euspen 19th Int. Conf.* 542-545
[6] Taniguchi N Nanotechnology 1996 Oxford Univ. Press
[7] ISO 230-1 2012